

# UC Berkeley

## UC Berkeley Previously Published Works

### Title

Influence of Macrocyclization on Allosteric, Juxtamembrane-Derived, Stapled Peptide Inhibitors of the Epidermal Growth Factor Receptor (EGFR)

### Permalink

<https://escholarship.org/uc/item/9zb2m25p>

### Journal

Organic Letters, 16(18)

### ISSN

1523-7060

### Authors

Sinclair, Julie K-L  
Schepartz, Alanna

### Publication Date

2014-09-19

### DOI

10.1021/ol502426b

Peer reviewed

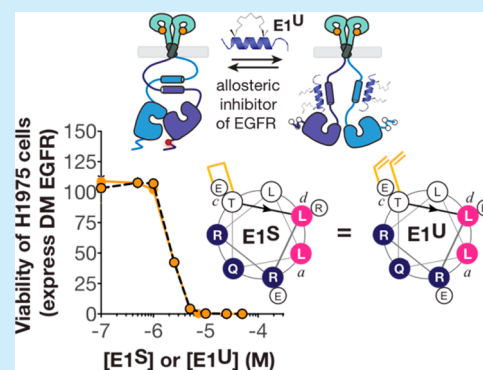
# Influence of Macrocyclization on Allosteric, Juxtamembrane-Derived, Stapled Peptide Inhibitors of the Epidermal Growth Factor Receptor (EGFR)

Julie K.-L. Sinclair<sup>†</sup> and Alanna Schepartz<sup>\*,†,‡</sup>

<sup>†</sup>Department of Chemistry and <sup>‡</sup>Department of Molecular, Cellular and Developmental Biology, Yale University, New Haven, Connecticut 06520-8107, United States

## S Supporting Information

**ABSTRACT:** The hydrocarbon-stapled peptide E1<sup>S</sup> allosterically inhibits the kinase activity of the epidermal growth factor receptor (EGFR) by blocking a distant but essential protein–protein interaction: a coiled coil formed from the juxtamembrane segment (JM) of each member of the dimeric partnership.<sup>1</sup> Macrocyclization is not required for activity: the analogous unstapled (but alkene-bearing) peptide is equipotent in cell viability, immunoblot, and bipartite display experiments to detect coiled coil formation on the cell surface.



Recently we reported<sup>1</sup> a group of hydrocarbon-stapled peptides<sup>2</sup> that allosterically inhibit the kinase activity of the epidermal growth factor receptor<sup>3</sup> (EGFR). The molecules we described block a protein–protein interaction distal to the kinase domain that is nonetheless essential for kinase function.<sup>4,5</sup> Specifically, these molecules block assembly of an antiparallel coiled coil containing the juxtamembrane (JM) segment from each member of the dimeric receptor partnership (Figure 1A).<sup>1</sup> Formation of the antiparallel JM coiled coil is conformationally coupled to assembly of the catalytically active asymmetric kinase dimer.<sup>4,6</sup> The most potent molecule we described, E1<sup>S</sup>, contains the sequence from the EGFR JM-A region (residues 650 to 666),<sup>1</sup> constrained by an *i* to *i* + 7 macrocyclic cross-link between residues 5 and 12 (654 and 661 according to EGFR numbering) (Figure 2A). In E1<sup>S</sup>, the cross-link lies at position “*c*” of the heptad repeat, on the helix face opposite the “*a*” and “*d*” positions used for coiled coil formation within intact EGFR dimers.<sup>4</sup> E1<sup>S</sup> decreases the viability of EGFR-dependent cell lines, inhibits EGFR autophosphorylation, and blocks coiled coil formation in live cells.<sup>1</sup> Here we report that macrocyclization *per se* is not required for any of these metrics: the analogous unstapled (but alkene-bearing) peptides are equipotent in cell viability, immunoblot, and bipartite tetracysteine display<sup>6,7</sup> experiments that monitor coiled coil formation within the JM on the mammalian cell surface.

In our previous work we noticed that the inhibitory potency of a JM-derived stapled peptide in cell-based proliferation assays was highly dependent on the location and identity of the macrocyclic cross-link. Although at least three molecules prepared previously (E1<sup>S</sup>, E2<sup>S</sup>, T4<sup>S</sup>) contained a cross-link

that should permit formation of a coiled coil dimer with a single EGFR JM segment, only one (E1<sup>S</sup>) was highly active.<sup>1</sup> We prepared a series of E1<sup>S</sup> variants to investigate this structure–activity relationship further (Figure 2A and Figure S1–2). One variant (JM<sup>Aib</sup>) contained a pair of  $\alpha$ -helix-promoting<sup>8</sup>  $\alpha$ -aminoisobutyric acid (Aib) residues at positions 5 and 12, replacing the alkene-bearing residues required for macrocyclization of E1<sup>S</sup>. JM<sup>Aib</sup> thereby decouples the functional contribution of  $\alpha$ -carbon quarternization and macrocyclization. A second, “unstapled” variant (E1<sup>U</sup>) contained the alkene-bearing residues required for macrocyclization of E1<sup>S</sup>, but no macrocyclization reaction was performed. Analogous “unstapled” versions of the remaining stapled peptides reported previously<sup>1</sup> (E2<sup>U</sup>, E4<sup>U</sup>, T1<sup>U</sup>, and T4<sup>U</sup>) were also prepared (Figure 1B), as were three new, stapled peptides (E2.2<sup>S</sup>, T4.2<sup>S</sup>, and E2.3<sup>S</sup>, Figure 1C) designed to further probe the role of staple placement on EGFR inhibition. Two new molecules, E2.2<sup>S</sup> and T4.2<sup>S</sup>, contain a single *i* to *i* + 3 cross-link that is displaced by one helix turn from its position in E2<sup>S</sup> and T4<sup>S</sup>, respectively; the last, E2.3<sup>S</sup>, contains an *i* to *i* + 7 cross-link (like E1<sup>S</sup>) between residues located at two *f* positions of the heptad repeat.

As expected,<sup>9</sup> when examined using circular dichroism (CD) spectroscopy all unstapled peptides displayed more  $\alpha$ -helix content than JM<sup>WT</sup> or JM<sup>Aib</sup> but less than the analogous stapled molecules. The ellipticity values at 222 nm ( $\epsilon_{222}$ ) of E1<sup>U</sup>, E2<sup>U</sup>, E4<sup>U</sup>, T1<sup>U</sup>, and T4<sup>U</sup> all fall between  $-9000$  and  $-15\,700$  deg $\cdot$ cm<sup>2</sup>·dmol<sup>-1</sup> with E4<sup>U</sup> at the low (less structured) end and E2<sup>U</sup>

Received: August 15, 2014

Published: September 10, 2014

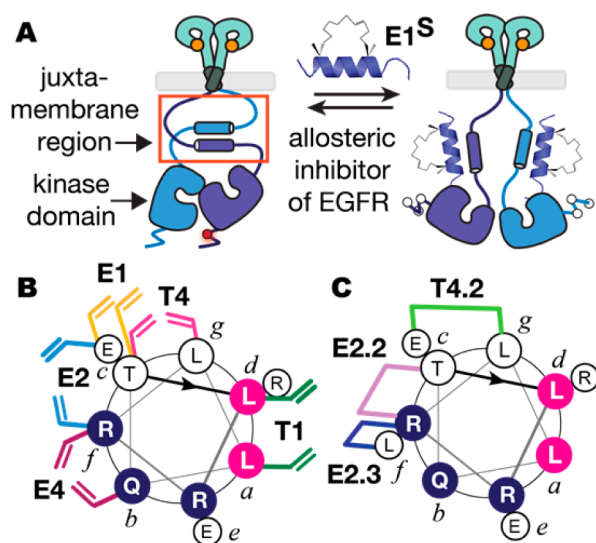


**Figure 1.** (A) Scheme illustrating the proposed interaction of the hydrocarbon-stapled peptide<sup>2</sup> E1<sup>S</sup> with the EGFR juxtamembrane (JM) segment to inhibit coiled coil formation between two receptor monomers and thus kinase activity.<sup>1</sup> Helical wheel representation of (B) unstapled alkene precursors to previously reported hydrocarbon-stapled peptides E1<sup>S</sup>, E2<sup>S</sup>, E4<sup>S</sup>, T1<sup>S</sup>, and T4<sup>S</sup> and (C) three new, stapled variants of E1<sup>S</sup>.

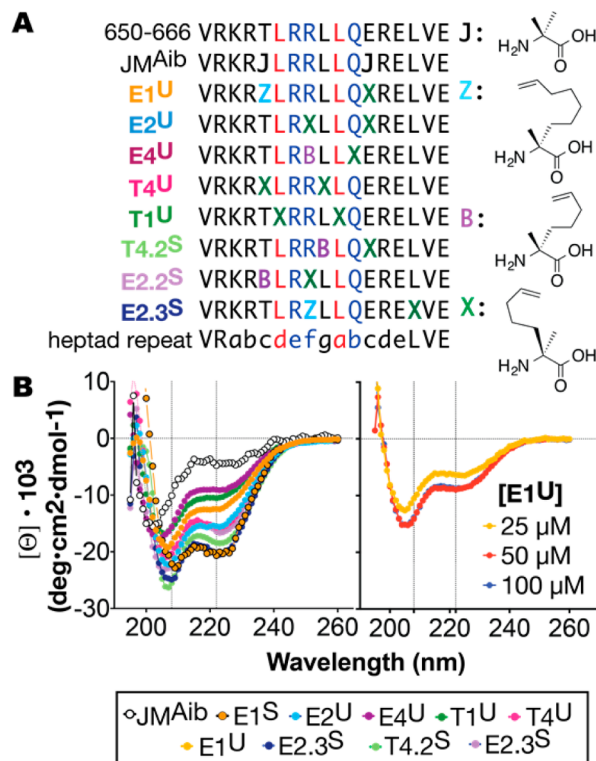


**Figure 2.** (A) Sequences and (B) circular dichroism (CD) spectra of of stapled and unstapled peptides studied herein. CD spectra of the indicated peptides at 25  $\mu$ M concentration in Dulbecco's phosphate buffered saline (dPBS); CD spectra of E1<sup>U</sup> at 25, 50, and 100  $\mu$ M. See also Figure S3.

and E4<sup>U</sup> at the high (more structured) end (Figures 2B and S3). The values reported for the analogous stapled molecules range from  $-15\,600$  to  $-20\,700$  deg·cm<sup>2</sup>·dmol<sup>-1</sup>.<sup>1</sup> Like the stapled variants, the  $\epsilon_{222}$  values of the unstapled peptides

increased little if at all in the 25 and 100  $\mu$ M concentration range (Figure S3), suggesting that all are predominantly monomeric at the lower concentrations employed (1 to 10  $\mu$ M).

Next we made use of five cell lines to evaluate the extent to which each E1<sup>S</sup> variant modulated the viability of EGFR-dependent cells. Four of the five cell lines express EGFR but differ in the EGFR mutational state; one line does not express EGFR (Figure 3). A431 and H2030 cells express wild type

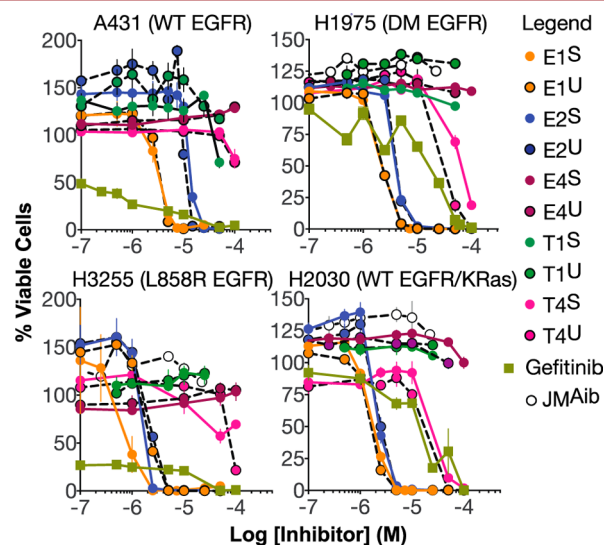


**Figure 3.** Effect of stapled and unstapled peptides on the viability of four EGFR-dependent cell lines. Each plot illustrates the % of viable cells remaining after 18 h of treatment with the [ligand] shown. Viability was assessed by monitoring oxyluciferin production by Ultra-Glo luciferase. Error bars show standard error of the mean. Data obtained using SK-N-MC cells, which do not express EGFR, are shown in Figure S4A. Data for E2.2<sup>S</sup>, E2.3<sup>S</sup>, and E4.2<sup>S</sup> are shown in Figure S4B–D.

EGFR, whereas H3255 and H1975 cells express single (L858R) or double (L858R/T790M) mutant forms, respectively; SK-N-MC cells express ErbB2–4 but not EGFR.<sup>10</sup>

The dose response curves in Figures 3 and S4 reveal several trends. First, as expected, cells expressing WT EGFR (A431) are sensitive to the small molecule tyrosine kinase inhibitor Gefitinib<sup>11</sup> and to the stapled peptides E1<sup>S</sup> and (less so) E2<sup>S</sup>, but not the stapled peptides E4<sup>S</sup>, T1<sup>S</sup>, and T4<sup>S</sup>, even at concentrations as high as 100  $\mu$ M.<sup>1</sup> Notably, the dose–response curves for the unstapled versions of E1<sup>S</sup> and E2<sup>S</sup> (E1<sup>U</sup> and E2<sup>U</sup>, respectively) are superimposable on those for the analogous stapled molecule. In fact, even the dose–response curves for the (virtually) inactive, stapled molecules (E4<sup>S</sup> and T4<sup>S</sup>) are superimposable on the analogous unstapled variants (E4<sup>U</sup> and T4<sup>U</sup>). The similarity in activity between stapled and unstapled analogs is especially surprising since the former are expected to possess longer half-lives *in cellulo* than the latter.<sup>12,13</sup> It is notable that the only sequence whose stapled and unstapled analogs behave differently is T1, where the staple replaces the leucine-rich interface required for formation of the proposed peptide:JM coiled coil.

The similarity between the effects of stapled and unstapled analogs are also apparent in H2030 and H1975 cells (Figure 3B,C) and the EGFR-deficient SK-N-MC cell line (Figure S4A): E1<sup>S</sup> and E1<sup>U</sup> are equipotent, as are E2<sup>S</sup> and E2<sup>U</sup>. The

only instance where a stapled peptide and its unstapled analog perform differently occurs in H3255 cells that express L858R EGFR, a constitutively active EGFR mutant that is sensitive to gefitinib and erlotinib. H3255 cells are 2-fold more sensitive to E1<sup>S</sup> than to E1<sup>U</sup>, perhaps because of mutation-induced differences in JM structure in these receptor variants. Although previous reports might predict that the unstapled analog of an active, stapled inhibitor would show diminished activity,<sup>13,14</sup> we find that E1<sup>S</sup> and E1<sup>U</sup> have nearly identical effects on the viability of these five cell lines.

We also evaluated the activity of three, new, stapled peptide variants of E1<sup>S</sup> and E2<sup>S</sup>. These molecules (E2.3<sup>S</sup>, E2.2<sup>S</sup>, and T4.2<sup>S</sup>) were chosen to provide additional information about the contribution of staple placement to inhibitor potency (Figure S4B–D). E2.3<sup>S</sup>, which like E1<sup>S</sup> carries an *i* to *i* + 7 cross-link on the helix face opposite that required for coiled coil formation, is inactive in all cell lines examined, whereas E2.2<sup>S</sup> and T4.2<sup>S</sup> are active at only the highest concentrations examined (IC<sub>50</sub> > 100 μM) and equally active in SK-N-MC cells that do not express EGFR (Figure S4A). Taken as a whole, the lack of activity displayed by E2.3<sup>S</sup>, E2.2<sup>S</sup>, and T4.2<sup>S</sup> indicates that position “*c*” of the heptad repeat is privileged with respect to inhibiting EGFR in these cell lines. This observation may reflect the requirement for multiple α-helix faces or binding modes; further work on this front is in progress.

In our previous work, we performed immunoblotting experiments to monitor the effect of each stapled peptide on the phosphorylation of EGFR and the downstream factors Akt and Erk in A431 cells.<sup>1</sup> The stapled peptide E1<sup>S</sup> caused a dose-dependent decrease in EGFR autophosphorylation at several positions within the C-terminal tail. E1<sup>S</sup> inhibited phosphorylation at Y845, Y1045, Y1086, and Y1173, but not Y1068 and Y1148. A431 cells treated with E1<sup>S</sup> also showed decreased levels of phospho-Akt and phospho-Erk, whereas the levels of EGFR, Akt, and Erk themselves were unaffected.<sup>1</sup>

Treatment of A431 cells with an equivalent concentration of E1<sup>U</sup> led to a pattern of phosphorylation changes within EGFR, Akt, and Erk that was virtually identical to that seen with E1<sup>S</sup> (Figure 4). The only detectable difference between the effects of E1<sup>S</sup> and E1<sup>U</sup> is the relative decrease in phosphorylation of Y1173. In cells treated with E1<sup>S</sup>, the level of phosphorylated Y1173 is downregulated more than in cells treated with E1<sup>U</sup>. Thus, in A431 cells, the effects of E1<sup>S</sup> and E1<sup>U</sup> on EGFR signaling are virtually identical; the small difference in α-helicity

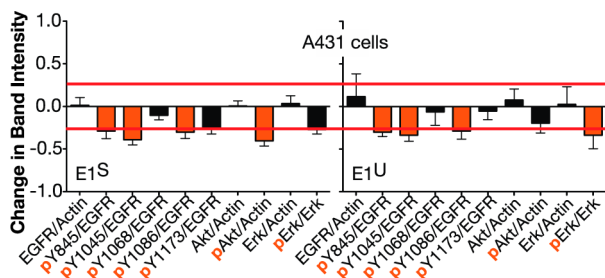


**Figure 4.** Comparison of the effects of E1<sup>S</sup> and E1<sup>U</sup> on EGFR autophosphorylation and on phosphorylation of Akt and Erk1/2. A431 cells were treated with 10 μM of either E1<sup>S</sup> or E1<sup>U</sup> for 1 h, stimulated with 10 ng/mL EGF, and then lysed, immunoblotted, and visualized. Plots show the decrease in intensity of the indicated phospho-protein band relative to untreated cells. Error bars represent the standard error of the mean over at least four trials. Immunoblots of A431 cells treated with E2.2<sup>S</sup>, T4.2<sup>S</sup>, and E2.3<sup>S</sup> are found in Figure S5.

observed *in vitro* (Figure 2) has no significant effect on EGFR inhibitory potency. E1<sup>S</sup>, E1<sup>U</sup>, T1<sup>S</sup>, T1<sup>U</sup>, E2.2<sup>S</sup>, and E4.2<sup>S</sup> all reached the cytosol of H2030 cells with comparable efficiencies when evaluated using the recently reported GIGT assay<sup>15</sup> (Figure S6), suggesting that, in these cases, the presence of a lipophilic side chain contributes more to permeability than does macrocyclization *per se*.

The experiments described above suggest that E1<sup>U</sup>, like E1<sup>S</sup>, allosterically inhibits the kinase activity of EGFR, presumably through an interaction with the distal juxtamembrane segment (Figure 1). To evaluate whether the mode of inhibition by E1<sup>U</sup> also mimics that of E1<sup>S</sup>,<sup>1</sup> we made use of a validated bipartite tetracysteine display assay<sup>6,7,16</sup> to determine whether E1<sup>U</sup> would also inhibit JM coiled coil formation within full length EGFR dimers expressed on the cell surface. CHO-K1 cells that transiently expressed the CysCys EGFR variant CC<sub>H</sub>-1 (whose cysteine arrangement in the paired EGF-induced dimer supports ReAsH binding and fluorescence)<sup>6</sup> were exposed individually to E1<sup>S</sup> and E1<sup>U</sup> as well as JM<sup>Aib</sup>, stimulated with EGF, and incubated with ReAsH, and the fluorescence increase due to ReAsH was quantified using total internal reflectance fluorescence microscopy (TIRF-M) (Figure 5). Treatment with

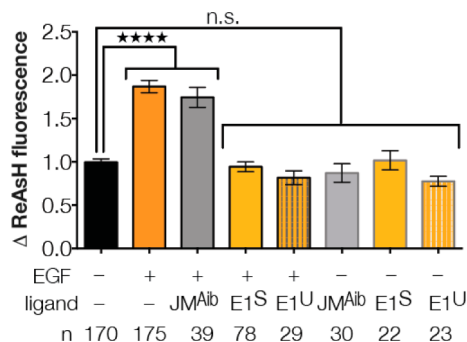


**Figure 5.** Comparison of the effects of E1<sup>S</sup> and E1<sup>U</sup> on formation of the EGF-induced coiled coil within the EGFR JM using TIRF-M and bipartite tetracysteine display. CHO-K1 cells were transfected with plasmid encoding EGFR CC<sub>H</sub>-1,<sup>6</sup> treated with 1 μM of the indicated ligand for 1 h, stimulated in the presence or absence of 100 ng/mL EGF for 30 min, and labeled with ReAsH. The plot illustrates the change in ReAsH fluorescence at 568 nm of *n* CHO-K1 cells relative to the level of EGFR expression. Error bars represent the standard error of the mean: \*\*\*\**p* < 0.01, \*\*\*\**p* < 0.0001; one-way ANOVA with Bonferroni postanalysis accounting for multiple comparisons.

EGF alone led to the expected increase in ReAsH fluorescence at the cell surface; this increase was unchanged by the presence of JM<sup>Aib</sup>. However, treatment of cells with 1 μM E1<sup>S</sup> or E1<sup>U</sup> led to a significant loss in ReAsH fluorescence. Neither E1<sup>S</sup> nor E1<sup>U</sup> affected ReAsH fluorescence in the absence of EGF (Figure 5). We conclude that E1<sup>U</sup>, like E1<sup>S</sup>, inhibits the intradimer coiled coil required for assembly of the active asymmetric kinase dimer. Like E1<sup>S</sup>, E1<sup>U</sup> is an allosteric inhibitor of EGFR. Experiments to identify the precise binding site(s) of E1<sup>S</sup> and E1<sup>U</sup> are in progress and will be reported in due course.

## ■ ASSOCIATED CONTENT

### Supporting Information

Experimental procedures and data. This material is available free of charge via the Internet at <http://pubs.acs.org>.

**■ AUTHOR INFORMATION****Corresponding Author**

\*E-mail: Alanna.schepartz@yale.edu.

**Notes**

The authors declare no competing financial interest.

**■ ACKNOWLEDGMENTS**

We gratefully acknowledge the NIH for support of this work (GM 83257).

**■ REFERENCES**

- (1) Sinclair, J. K. L.; Denton, E. V.; Schepartz, A. *J. Am. Chem. Soc.* **2014**, *136*, 11232–11235.
- (2) Verdine, G. L.; Hilinski, G. J. *Drug Discovery Today* **2012**, *9*, e41–e47. Walensky, L. D.; Kung, A. L.; Escher, I.; Malia, T. J.; Barbuto, S.; Wright, R. D.; Wagner, G.; Verdine, G. L.; Korsmeyer, S. J. *Science* **2004**, *305*, 1466–1470. Moellering, R. E.; Cornejo, M.; Davis, T. N.; Del Bianco, C.; Aster, J. C.; Blacklow, S. C.; Kung, A. L.; Gilliland, D. G.; Verdine, G. L.; Bradner, J. E. *Nature* **2009**, *462*, 182–U57. Walensky, L. D.; Bird, G. H. *J. Med. Chem.* **2014**, *57*, 6275–6288.
- (3) Taylor, J. M.; Mitchell, W. M.; Cohen, S. *J. Biol. Chem.* **1974**, *249*, 2188–2194. Cohen, S.; Carpenter, G.; King, L. *J. Biol. Chem.* **1980**, *255*, 4834–4842.
- (4) Jura, N.; Endres, N. F.; Engel, K.; Deindl, S.; Das, R.; Lamers, M. H.; Wemmer, D. E.; Zhang, X.; Kuriyan, J. *Cell* **2009**, *137*, 1293–1307.
- (5) He, L.; Hristova, K. *Sci. Rep.* **2012**, *2*, 854. Brewer, M. R.; Choi, S. H.; Alvarado, D.; Moravcevic, K.; Pozzi, A.; Lemmon, M. A. *Mol. Cell* **2009**, *34*, 641–651.
- (6) Scheck, R. A.; Lowder, M. A.; Appelbaum, J. S.; Schepartz, A. *ACS Chem. Biol.* **2012**, *7*, 1367–1376.
- (7) Luedtke, N. W.; Dexter, R. J.; Fried, D. B.; Schepartz, A. *Nat. Chem. Biol.* **2007**, *3*, 779–784.
- (8) Burgess, A. W.; Leach, S. J. *Biopolymers* **1973**, *12*, 2599–2605. Marshall, G. R.; Hodgkin, E. E.; Langs, D. A.; Smith, G. D.; Zabrocki, J.; Leplawy, M. T. *Proc. Natl. Acad. Sci. U.S.A.* **1990**, *87*, 487–491.
- (9) Schafmeister, C. E.; Po, J.; Verdine, G. L. *J. Am. Chem. Soc.* **2000**, *122*, 5891–5892.
- (10) Kawamoto, T.; Sato, J. D.; Le, A.; Polikoff, J.; Sato, G. H.; Mendelsohn, J. *Proc. Natl. Acad. Sci. U.S.A.* **1983**, *80*, 1337–1341. Fallon, K.; Havlioglu, N.; Hamilton, L.; Cheng, T. H.; Carroll, S. J. *Neuro-Oncol.* **2004**, *66*, 273–284. Pao, W.; Miller, V. A.; Politi, K. A.; Riely, G. J.; Somwar, R.; Zakowski, M. F.; Kris, M. G.; Varmus, H. *PLoS Med.* **2005**, *2*, 0225–0235. Aifa, S.; Aydin, J.; Nordvall, G.; Lundström, I.; Svensson, S. P. S.; Hermanson, O. *Exp. Cell Res.* **2005**, *302*, 108–114.
- (11) Ciardiello, F. *Drugs* **2000**, *60*, 25–32.
- (12) Bird, G. H.; Madani, N.; Perry, A. F.; Princiotta, A. M.; Supko, J. G.; He, X. Y.; Gavathiotis, E.; Sodroski, J. G.; Walensky, L. D. *Proc. Natl. Acad. Sci. U.S.A.* **2010**, *107*, 14093–14098. Shi, X. G.; Wales, T. E.; Elkin, C.; Kawahata, N.; Engen, J. R.; Annis, D. A. *Anal. Chem.* **2013**, *85*, 11185–11188.
- (13) Giordanetto, F.; Revell, J. D.; Knerr, L.; Hostettler, M.; Paunovic, A.; Priest, C.; Janefeldt, A.; Gill, A. *ACS Med. Chem. Lett.* **2013**, *4*, 1163–1168.
- (14) Long, Y.-Q.; Huang, S.-X.; Zawahir, Z.; Xu, Z.-L.; Li, H.; Sanchez, T. W.; Zhi, Y.; De Houwer, S.; Christ, F.; Debyser, Z.; Neamati, N. *J. Med. Chem.* **2013**, *56*, 5601–5612. Bernal, F.; Tyler, A. F.; Korsmeyer, S. J.; Walensky, L. D.; Verdine, G. L. *J. Am. Chem. Soc.* **2007**, *129*, 2456–2457.
- (15) Appelbaum, J. S.; LaRochelle, J. R.; Smith, B. A.; Balkin, D. M.; Holub, J. M.; Schepartz, A. *Chem. Biol.* **2012**, *19*, 819–830. Holub, J. M.; LaRochelle, J. R.; Appelbaum, J. S.; Schepartz, A. *Biochemistry* **2013**, *52*, 9036–9046.
- (16) Scheck, R. A.; Schepartz, A. *Acc. Chem. Res.* **2011**, *44*, 654–665.